Content available at: https://www.ipinnovative.com/open-access-journals

International Journal of Clinical Biochemistry and Research

Journal homepage: www.ijcbr.in

Original Research Article

Decoding the enigma of bursal disease virus: Unraveling the complex interactions of proteins and molecules for enduring stability

Muhammad Danish Mehmood[1]*, Ehsan Ali[2], Huma Anwar Ul-Haq[1], Rabia Habib[1], Muhammad Ismail[1], Fareeha Arshed[3]

[1]Ottoman Pharma Immuno Division, Lahore, Pakistan.
[2]The Islamia University of Bahawalpur, Pakistan.
[3]Riffah International University, Lahore Campus, Lahore Pakistan.

Abstract

The project aimed to evaluate ten Indigenous isolates of the Infectious Bursal Disease (IBD) virus using in silico methodologies, including phylogenetic analysis, homology modelling, and molecular dynamics simulations. The study focused on understanding the physiological and chemical properties of the viral surface target proteins, the interactions between proteins and ligands, and the stability of various protein-ligand complexes. The results revealed differences in stability and interaction patterns among the complexes, highlighting the significance of specific residues and secondary structural elements. These findings provide valuable insights into the behavior of the viral isolates and their potential impact on Bursal Disease. The abstract emphasizes the need for future research to build on these findings to enhance our understanding of IBD genetic diversity and improve disease control measures by developing effective homologous vaccines.

Keywords: Infectious Bursal Disease virus (IBD), Phylogenetic analysis, 3D protein structure, Molecular Docking

Received: 13-01-2025; **Accepted:** 18-02-2025; **Available Online**: 22-03-2025

1. Introduction

The challenge of infectious bursal disease (IBD) is substantial in the ongoing effort to develop an effective vaccine against emerging and frequently encountered contagious diseases.[1,23] IBD is instigated by the infectious bursal disease virus (IBDV), also recognized as Gumboro disease. This double-stranded RNA virus is categorised within the family Birnaviridae and the genus Avibirnavirus. This acute, highly transmissible, and immunosuppressive ailment primarily impacts young chickens aged between 3 and 6 weeks, while older birds may exhibit a subclinical manifestation of the infection.[2,9]

In the context of commercial poultry farming, a variety of infections can be introduced into the environment by birds, posing a significant threat to the industry.[3] IBDV gravely undermines the growth of the global chicken market and results in considerable financial setbacks (Sharma *et al*., 2000). There are two recognized serotypes of IBDV, with only serotype I viruses posing a threat to chickens. The IBDV genome comprises two segments, A and B. Segment A encompasses two partially overlapping larger and smaller open reading frames (ORFs), contributing to the virulence and pathogenicity of the virus.[5]

Infection with infectious bursal disease virus (IBDV) is recognised for its substantial impact on local and humoral immune responses.[6] The highly virulent strain of IBDV (vvIBDV) has a specific affinity for B lymphocytes, leading to immunosuppression and increased mortality rates in young birds. This strain also inflicts damage on primary lymphoid organs, including the bursa of Fabricius, spleen, thymus, and cecal tonsils.[7] Notably, IBDV exhibits high stability,

*Corresponding author: Muhammad Danish Mehmood
Email: danishmehmood@ottomanpharma.com

DOI: https://10.18231/j.ijcbr.2025.007

persisting in chicken houses even after extensive cleaning and disinfection. It demonstrates enhanced resistance to heat, UV light, and photodynamic inactivation compared to reoviruses.[8]

Effective management of IBD entails immunization, but the widespread use of live vaccines has contributed to the emergence of novel strains.[2] The virus's primary host-protective capsid protein, VP2, can induce neutralizing antibodies and carry immunogenic determinants. Recent studies have identified significant variations in the amino acids within the hyper-variable region of the capsid protein VP2 (hVP2) across different populations. Consequently, IBDV has been categorized into seven geno groups, with genogroup-1 prevalent worldwide.[10]

After extensive research, experts are still working on developing a specific vaccine, prompting them to seek new methods for vaccine innovation and advancement. They are striving to discover rapid, cost-effective, and precise vaccines. By integrating computational biology, bioinformatics, and molecular dynamics simulations, researchers hope to achieve this goal. In a recent study, bioinformatics tools were utilised to explore new approaches for designing a safe and effective bio-adjuvant candidate vaccine using the partial sequence of VP1, VP2, VP3, VP4, and VP5 protein isolates.[11,12]

2. Materials and Methods

2.1. Sample collection

Fabricius's bursa, spleen, and liver samples were obtained from birds suspected of being infected with the infectious bursal disease virus (IBDV) during a natural outbreak in a commercial white leghorn layer flocks reared in different areas of Pakistan. These samples were collected through post-mortem and utilized for virus isolation and molecular characterization.

2.2. Virus isolation

The processed bursa of fabric was exposed to virus isolation using primary chicken embryo fibroblast (CEF) cells. The CEF cells were prepared according to standard procedure and were infected with 10% bursal suspension for 1 hour at 37°C. The cultures were then placed in a CO_2 incubator at 37°C with a 5% CO_2 concentration and checked twice daily for cytopathic effects (CPE). Positive (vaccine virus) and negative controls were also included in the process.

2.3 Virus characterization

The process began with extracting viral RNA from infected fibroblast cells of IBDV-positive samples using a favorgen extraction kit. The extracted RNA was then used to produce the first strand of complementary DNA (cDNA) for the Polymerase Chain Reaction (PCR) using a transgenic kit. For Polymerase chain reaction (PCR), VP1-899bp and VP2-343bp sized partial VP gene of IBDV VP1-primer Forward: 5’ CAGCAGCGTCGGCATAAAGCCTAC 3’ and Reverse: 3'GTGGCACCCAGGGCTGTCATCCTCACC 5’ and VP2-primer Forward: 5'CAGGCCCAGAGAGTCTACACCAT3' and Reverse: 3’GGAGGTTACTATCTCCAGTTTG’5 were used. The PCR process involved filling 0.5 ml Eppendorf tubes with nuclease-free water, RNA template, and forward and reverse primers, followed by incubation and addition of reverse transcriptase, reverse transcriptase buffer and dNTPs. The cDNA reaction was then assembled and amplified for 30 minutes at 42˚C. The total volume was 25ul, in which 12ul master mix, 7ul nuclease-free water, 1 ul each forward and reverse prime, and 4ul DNA template were added. The DNA was amplified with an initial denaturation at 95°C for 5 minutes, denaturation at 95°C for 45 sec, annealing at 52°C for VP1 and 55°C for VP2 for 45 sec and extension at 72°C for 45 sec, followed by 30 cycles. The final extension was conducted in a Veritii thermocycler (Applied Biosystems-Thermo Fisher-USA) for 10 minutes at 72˚C. Subsequently, gel electrophoresis (Major Science-Taiwan) and band visualisation were performed using a UV trans illuminator (Vilber Lourmat-France).

2.3. Phylogenetic analysis

For sequencing, the PCR amplicon was shipped to Apical Scientific SDN. BHD. in Malaysia. Each sequence was compared with other specific comparable sequences submitted to the National Center for Biotechnology Information (NCBI) using a Basic Local Alignment Search Tool (BLAST) search. A maximum likelihood phylogenetic tree was built using the Clustal Omega alignment technique in MEGA (Molecular Evolutionary Genetics Analysis 11 Software) for the phylogenetic comparison. The phylogenetic tree was styled and coloured using iTol.

2.4. Target identification

The chicken bursa libraries contain 15546 genes. Six genes have been confirmed using quantitative reverse transcription-PCR. [13] IBDV genomes comprise two segments, A and B. Segment A contains two open reading frames (ORFs), one of which encodes a polyprotein cleaved by proteases to produce VP2, VP3, and VP4. VP2 is the primary antigen that protects IBDV. Segment B encodes the sole RNA-dependent RNA polymerase (VP1), responsible for replicating the viral genome (XU *et al*., 2019).[14]

3. Protein Selection and Structural Refinement

The UniProt database was used to obtain protein sequences in FASTA format. Expasy ProtPaaram was then utilised to predict the secondary structure and compute the physiochemical properties of the proteins, which aid in predicting their functions. Modellar 9,25 was used to estimate the protein's three-dimensional structure, and Pymol was utilised to visualise the proteins.[15]

4. Selection and Retrieval of Ligand

Based on information from PubChem and a literature survey, the biological activity of TLR 7/8 and chemical compounds from *Withania somnifera* were considered ligands. The 2D chemical structure was obtained using Pymol and then transformed into 3D.[16]

4.1. Docking analysis

The docking data generated using Pyrx software provided information about the binding affinities. The protein-ligand complex was analysed using PyMOL to identify the binding locations of the target protein and understand the interactions between the inhibitor and receptor.

4.2. Toxicity analysis

After examining the docking results, Swiss ADME was used to assess the drug's likeness and toxicity. This software helps identify key drug-like characteristics and forecast lead likeness.[17] Allertop and Vaxijan online tools were used to check the protein's antigenicity and allergenicity.

4.3. Lead identification

The most active inhibitors were identified based on docking score, ligand-protein interactions, and toxicity analysis. The compounds showing the least binding affinity, high lead likenesses, and best interactions were selected as potential inhibitors.

5. Molecular Dynamics Simulation

Molecular dynamics simulations were performed using the Desmond package for 20 nanoseconds. Protein-ligand complexes obtained through docking experiments were optimized and minimized using the Protein Preparation Wizard or Maestro. The simulation used a TIP3P solvent model with an orthorhombic box and OPLS_2005 force field. Counter ions and 0.15 M salt (NaCl) were added to neutralize the models and simulate physiological conditions. The simulation maintained a constant number of particles, pressure (1 atm), and temperature (300K). Trajectories were saved every 50 ps for analysis, and stability was evaluated using root mean square deviation (RMSD) of the protein and ligand over time.

6. Results

The study obtained five indigenous isolates of the IBDV for genomic analysis and compared them with reference national and international isolates. The protein accession numbers of the isolates are OP1 (WMM64994), OP2 (MM64995), OP3 (XBR33698), OP4 (XCI54779) and OP5 (XCI54780). The study found that OP3, OP4, and OP5 share a common region, indicating similarity among these three isolates. On the other hand, OP1 and OP2 are present in different regions from the other three isolates, suggesting differences in their genetic makeup, as depicted in **Figure 1**. The nucleotide accession numbers for the isolates are OP1 (OR166261), OP2 (OR166262), OP3 (PP857841), OP4 (PP966925), and OP5 (PP966926). The clade value of the nucleotide isolates is (0.01019576) OP2-VP1, OP1, OP3, OP4, and OP5 (VP2) values (0.00000325). The value indicates that OP1, OP3, OP4, and OP5 are in the same region and have similarities. In contrast, OP2 (VP1) has a different clade value from the other four isolates, showing no similarity with the other four, as shown in **Figure 2**.

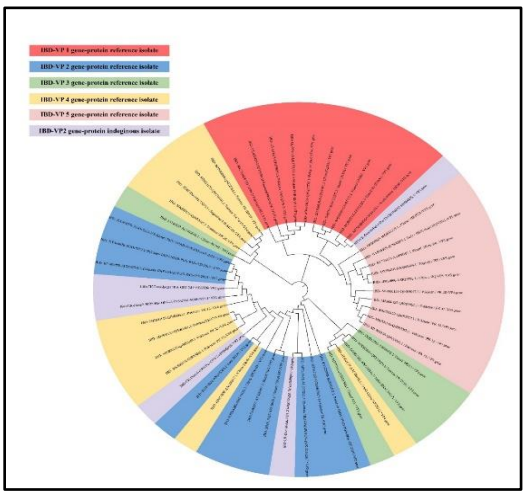

Figure 1: The phylogenetic tree of VP1 and VP2 IBDV Indigenous and reference amino acid isolates was constructed using the maximum likelihood method and aligned with clustal omega. It illustrates the genetic relationship among isolates. Each clade is color-coded to represent a specific VP gene group.

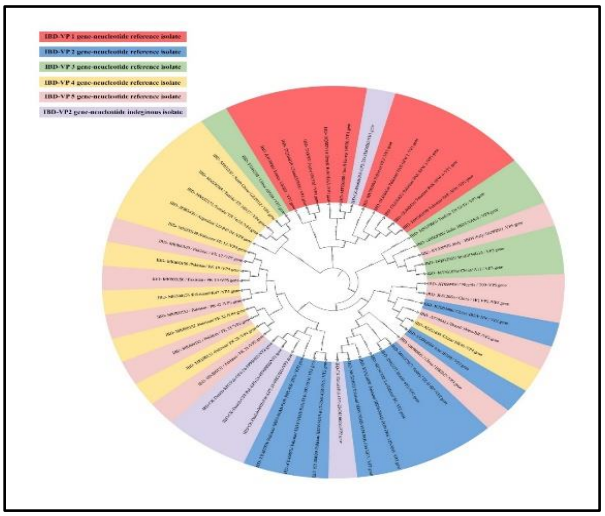

Figure 2: The phylogenetic tree of VP1 and VP2 IBDV Indigenous and reference nucleotide isolates was constructed using the maximum likelihood method and aligned with clustal omega. It illustrates the genetic. relationship among isolates. Each clade is color-coded to represent a specific VP gene group.

Based on similarities, a small list of isolates was created. The isolates OP1-VP2, OP2-VP1, and OP3-VP2 were anticipated

to have a 3D structure. Using modeller 9.25, I-TASSER, and trRosetta, homology modelling was used to create the protein's structure. For the particular protein, all methods produce the same outcome; neither structural nor functional alterations were made, as indicated in **Figure 3**, and **Figure 4**.

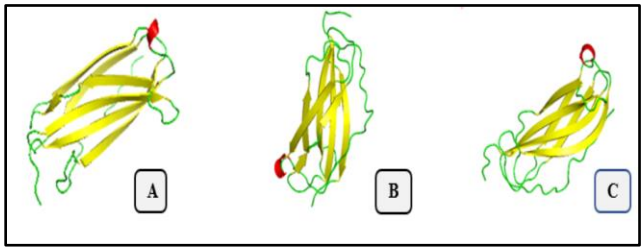

Figure 3: 3D VP2 protein structure of infectious bursal disease virus OP1 Accession OR166261 through **A:** Homology modelling, **B:** Ab initio (Rosetta) and **C:** Threading (I-taser).

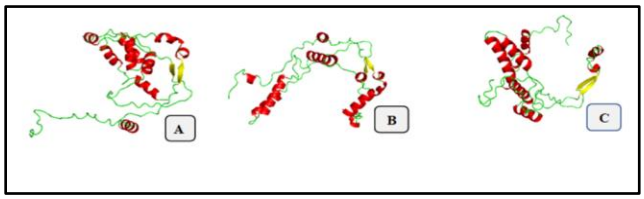

Figure 4: 3D VP1 protein structure of infectious bursal disease virus OP2 Accession OR166262 through **A:** Homology modelling, **B:** Ab initio (Rosetta) and **C:** Threading (I-taser).

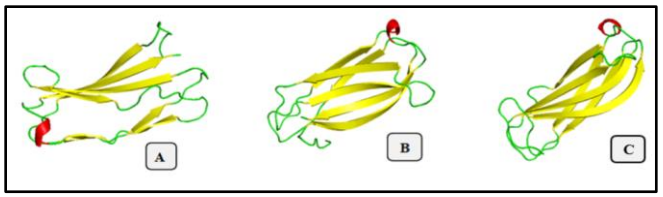

Figure 5: 3D VP2 protein structure of infectious bursal disease virus OP3 Accession PP857841 through **A:** Homology modelling, **B:** Ab initio (Rosetta) and **C:** Threading (I-taser).

The 3D structures from homology modelling were selected for further analysis. OP1-VP2's estimated structure consists of one helix and six sheets. OP1-VP2 had 118 total amino acid residues and a molecular weight of 12344.01. OP2-VP1 had 207 residues of amino acids and a molecular weight of 23308.72. OP2-VP1 has two sheets and nine helices. The OP3-VP2's data indicate that it has eight sheets and one helix. There are 99 residues of amino acids overall, and the molecular weight is 10189.64. 3D protein structures predicted from all techniques are shown in **Figure 3**, **Figure 4** and **Figure 5**.

7. Physiochemical Properties

The physiochemical properties of each 3D protein structure are evaluated using Expasy Prot—param, as shown in. The table describes the extinction coefficient, half-life, instability index, aliphatic index, and GRAVY. Extinction coefficients (εpercent) for proteins typically fall between 4.0 and 24.0. A protein is predicted to be stable if its instability index is less than 40, while values above 40 indicate it may be unstable. The standard value for the aliphatic index ranges from 66.5 to 84.33. The hydropathy value for each residue is added, and the result is divided by the sequence length to determine the GRAVY value.

The value of the extinction coefficient of OP1-VP2 is 0.483, OP3-VP2 is 0.292, and OP2-VP1 is 1.347. These do not pass the extinction coefficient analysis. The second property that Expasy Prot. Param provides the half-life. The half-life analysis predicts that OP2-VP1 has the best half-life with 30 hours (mammalian) in vitro, 20 hours (yeast) in vivo and 10 hours (E. coli) in vivo. At the second number, OP3-VP2 has a good half-life compared to OP1-VP2. The half-life of OP3-VP2 is 1.9 hours (mammalian) in vitro, 20 hours (yeast) in vivo and 10 hours (E. coli) in vivo. OP1-VP2 half-life is 1 hour (mammalian) in-vitro, 2 min (yeast) in-vivo and 2 min (Escolar) in-vivo. The value of OP1-VP2 for the half-life needs to be better. The third property is the instability index. It tells how much a protein is stable. OP1-VP2, with a value of 19.72, is stable, and OP3-VP2, with a value of 29.85, is also stable, while in the case of OP2-VP1, the value shows variation. The value of OP2-VP1 is 46.38, which makes it unstable and does not pass the stability analysis. The fourth property is the aliphatic index. OP1-VP2, with a value of 109.07, and OP3-VP2, with a value of 120.20, do not pass the analysis. In the OP2-VP1 case, the value is slightly higher than the ideal value, making OP2-VP1 nearer to thermal stability than the other two, which have a value of 87.63. The fifth property is GRAVY, which tells which protein is hydrophobic or hydrophilic. The value of OP1-VP2 is 0.408, and OP3-VP2 has a value of 0.644, making both of them hydrophobic. On the other hand, OP2-VP1 is hydrophilic with a value of -0.528. The value in negative shows that the protein is hydrophilic, while in positive, it is hydrophobic, as illustrated in **Table 1**.

Table 1: Physiochemical properties of the 3D protein structure of IBD:

Properties	OP1-VP2	OP3-VP2	OP2-VP1
Extinction Co-efficient (Ideal Value=4 to 24)	No Trp residues Abs=0.1% 0.483 Ext. Coefficient=5960	No Trp residues Abs=0.1% 0.292 Ext. Coefficient=3140	Trp residue found Abs=0.1% 1.347 Ext. Coefficient=31400
Half-Life	One hr. (mammalian) in-vitro 2 min (yeast) in-vivo 2 min (*E. coli*) in-vivo	1.9 hrs. (mammalian) in-vitro 20 hrs. (yeast) in-vivo 10 hrs. (*E. coli*) in-vivo	30 hrs. (mammalian) in-vitro 20 hrs. (yeast) in-vivo Ten hrs. (*E. coli*) in-vivo
Instability Index	19.72 (Stable)	29.85 (Stable)	46.38 (Unstable)
Aliphatic Index (66.5 to 84.33)	109.07	120.20	87.63
Gravy	0.408 (Hydrophobic)	0.644 (Hydrophobic)	-0.528 (Hydrophilic)

8. Protein-Ligand Complex

In a molecular docking analysis, a protein-ligand complex was created. The VP2 protein used TLR 7/8 (Ligand ID: 52945312) as the ligand, while the VP1 protein used *Withania somnifera* (Ligand ID: 161671). The docking studies identified the optimal binding pockets for the VP2 and VP1 proteins, with the ligands binding to those locations. A total of 1661 molecules were generated during the docking process, and three compounds were shortlisted with binding affinities ranging from -8 to -11, as indicated in **Figure 6**.

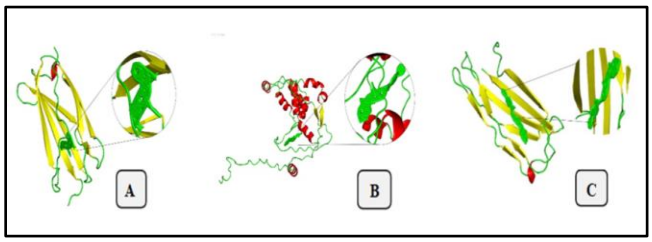

Figure 6: Capsid Protein structure and Ligand molecule complex of Indigenous isolates **A:** OP1-VP2 with TLR7/8; **B:** OP2-VP1 with *Withania somnifera* and **C:** OP3-VP2 with TLR7/8.

Were selected based on binding affinity. Ligands with values between -5.9 and -11 were shortlisted. Among them, two ligands were chosen with the best binding affinity, with values -10.6 and -10.5, and their 2D structure is displayed in **Figure 7**.

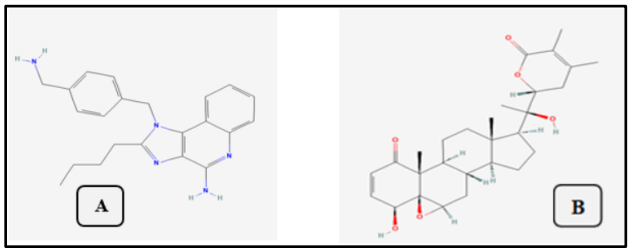

Figure 7: 2D structure of Ligand molecule Indigenous isolates **A:** TLR7/8 and **B:** *Withania somnifera*.

The Aller Top and VaxiJen tools were used to analyse the protein's allergen city and antigenicity. OP1-VP2 has been categorised as an allergen and an antigen, indicating that it can produce an immune response and allergic reactions. On the other hand, OP2-VP1 is neither an antigen nor an allergen, suggesting that it is unlikely to make an immunological response or an allergic reaction. As an antigen rather than an allergen, OP3-VP2 can elicit an immune response without triggering an allergic reaction. These results demonstrate the different immunological profiles of the proteins.

8.1 Molecular dynamics simulation of OP1-VP2

In the simulation time of 20 nanoseconds, OP1-VP2 shows good stability and interaction between the protein and ligands. The interaction between protein and ligand in the first 0.0 to 10.0 nanoseconds is outstanding. The interaction becomes weak in the next ten nanoseconds. This result is quite acceptable, as shown in **Figure 9**.

The protein's RMSF value, a key determinant of its stability, is influenced by its residue-wise binding to the ligand. Residues with higher peaks, typically found in loop regions identified from MD trajectories or N- and C-terminal zones, play a crucial role in this interaction. The low RMSF values of the binding site residues indicate the stability of the ligand binding to the protein.

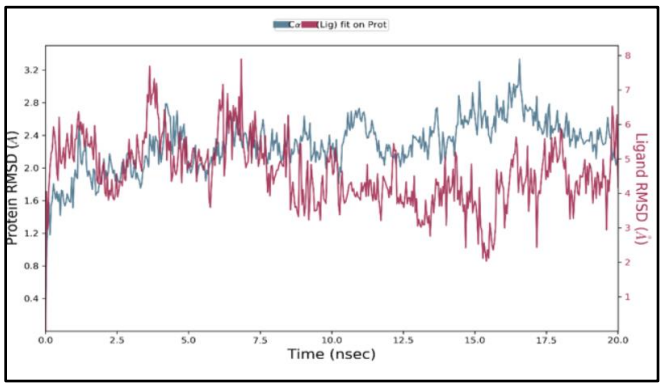

Figure 8: Root mean square deviation (RMSD) of the backbone atoms of protein and the ligand with time. The left Y-axis shows the variation of protein RMSD through time. The right Y-axis shows the variation of ligand RMSD through time.

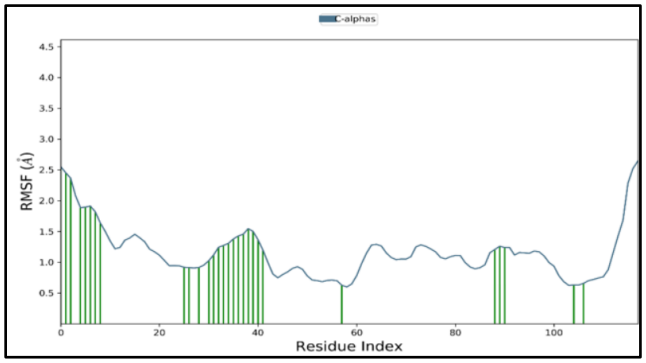

Figure 9: Residue-wise root mean square fluctuation (RMSF) of protein.

The protein-ligand contact histogram, a significant tool in our analysis, reveals most of the hydrophobic and hydrogen interactions between the protein and ligand, as depicted in **Figure 14**. TYR_3 and ILE_5 emerge as the most critical residues regarding hydrogen and hydrophobic interactions, underscoring their role in the protein-ligand interaction.

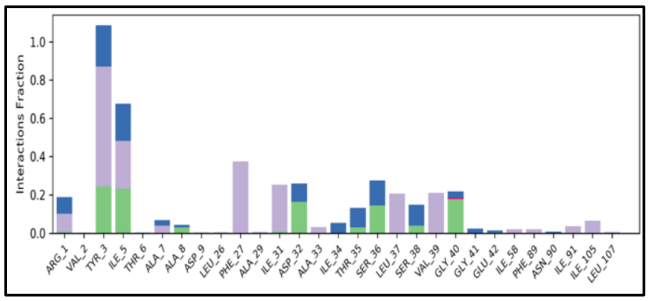

Figure 10: Protein-ligand contact histogram.

The percentage SSE graphs show that in OP1-VP2, beta strands are more prominent than the alpha helix. This can affect the protein's stability and functionality.

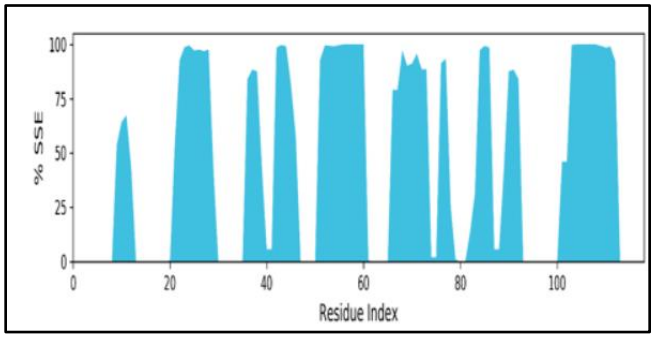

Figure 11: Protein secondary structure element distribution by residue index throughout the protein structure. Blue columns indicate beta-strands.

8.3 Molecular dynamics simulation of OP2-VP1

The simulation process of OP2-VP1 produced results different from those of (OP1-OP3) VP2. The RMSD graph shows that the Protein and ligand interact best in the first 0.0 to 2.5 nanoseconds. Protein and ligand are stable throughout the simulation, but their interaction is not better than that of OP1-VP2.

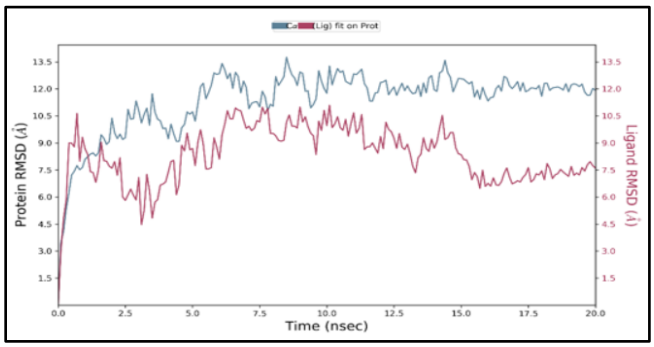

Figure 12: Root mean square deviation (RMSD) of the backbone atoms of protein and the ligand with time. The left Y-axis shows the variation of protein RMSD through time. The right Y-axis shows the variation of ligand RMSD through time.

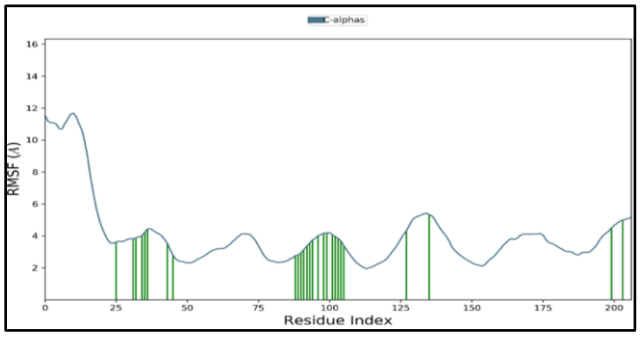

Figure 13: Residue-wise root mean square fluctuation (RMSF) of protein.

The percentage SSE graph of OP2-VP1 shows that the structure has more alpha helix than beta strands, which are essential to its stability.

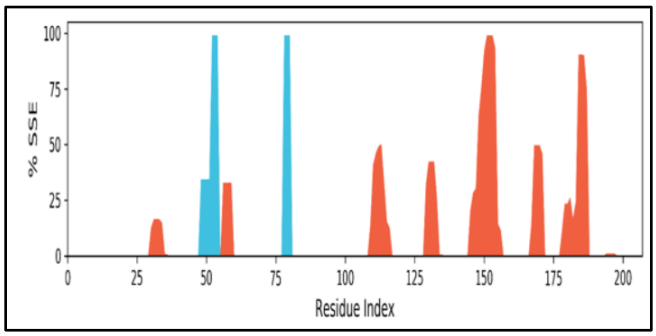

Figure 14: Protein Secondary Structure element distribution by residue index throughout the protein structure. Red columns indicate alpha helices, and blue columns indicate beta-strands.

The protein-ligand contact histogram shows most of the protein and ligand's hydrophobic and hydrogen interactions. TYR_92 is the most important in terms of hydrogen and hydrophobic interactions.

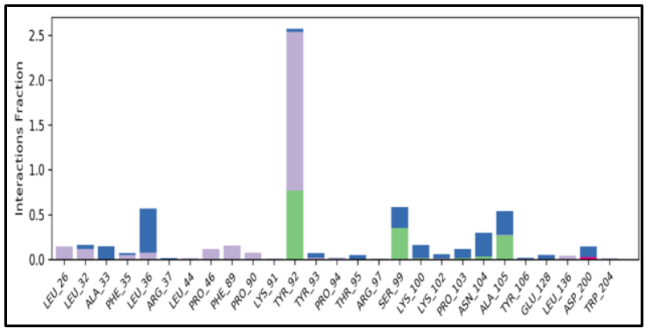

Figure 15: Protein-Ligand contact histogram.

The simulation results for the OP3-VP2 are different from those for the OP1-VP2 and OP2-VP1. During the 20-nanometer simulation, there is no interaction in the first 0.0 to 7 nanoseconds. Between 7.5 and 14 nanoseconds, the best interaction between protein and ligand occurs, making it stable.

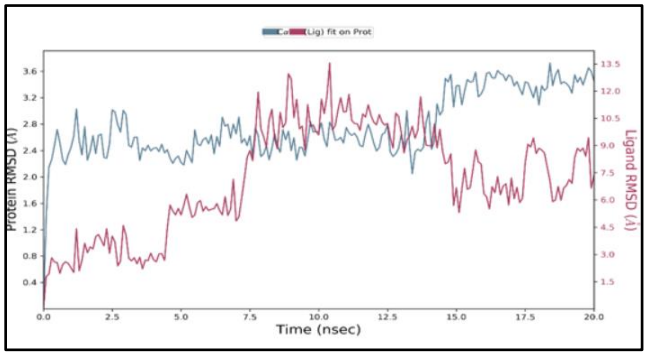

Figure 16: Root mean square deviation (RMSD) of the backbone atoms of protein and the ligand with time. The left Y-axis shows the variation of protein RMSD through time. The right Y-axis shows the variation of ligand RMSD through time.

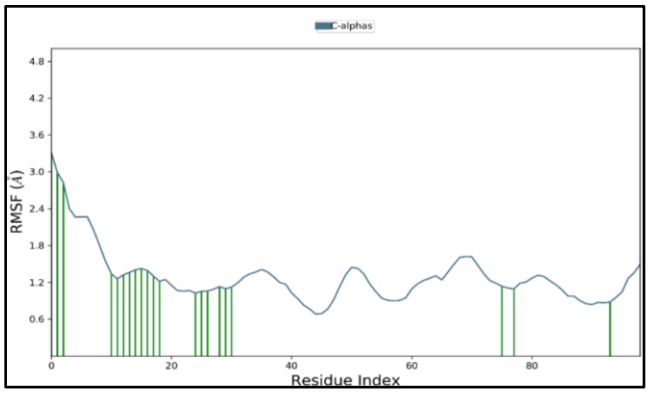

Figure 17: Residue-wise root mean square fluctuation (RMSF) of protein.

The percentage SSE graph shows OP3-VP2 has more beta strands than alpha helixes. The parentage SSE results of OP1-VP2 and OP3-VP2 are similar, while the OP2-VP1 percentage SSE graph shows an alpha helix.

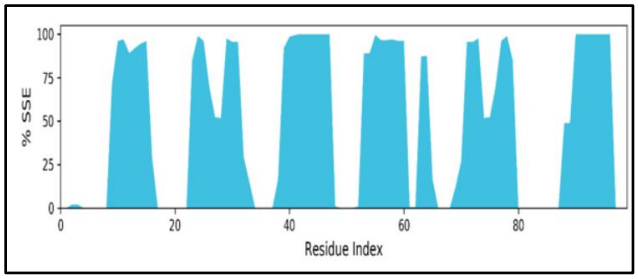

Figure 18: Protein Secondary Structure element distribution by residue index throughout the protein structure. Blue columns indicate beta-strands.

The protein-ligand contact histogram shows most of the hydrophobic and hydrogen interactions between the protein and ligand. GLY_27 is the most important in terms of hydrogen and hydrophobic interactions.
(OP1-OP3)VP2 AND OP2-VP1 all have hydrophobic and hydrogen interactions for the stability of the structure.

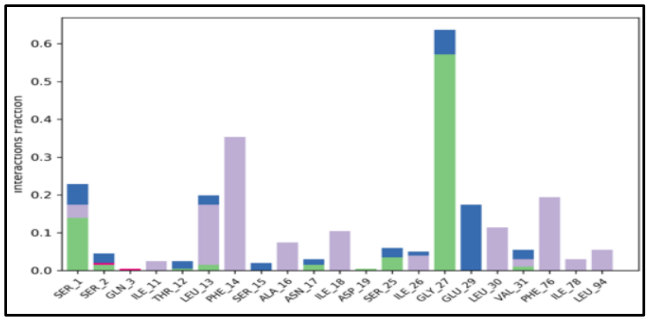

Figure 19: Protein-ligand contact histogram.

9. Discussion

Bioinformatics help in the vaccine development of IBD by analysing protein and gene data to find the potential target. It also analyses how the immune system will respond to the particular vaccine; current research aimed to identify and evaluate 10 Bursal Disease viral isolates using in silico methodologies such as phylogenetic analysis. Two phylogenetic trees were generated for the amino acid and nucleotide isolates of IBDV. The results showed that OP3, OP4, and OP5 isolates share a common region, indicating similarity, while OP1 (VP2) and OP2 (VP1) are in different areas. The clade values for the amino acid isolates were (0.01640571) OP1–VP2, (0.00972679) OP2-VP1, and (0.00000103) OP3, OP4, OP5 (VP2) (Liu *et al*., 2011).

The clade value of the nucleotide isolates is 0.01019576 for OP2-VP1, OP1, OP3, OP4, and OP5, while the value for OP2 (VP2) is 0.00000325. The analysis indicates that OP1, OP3, OP4, and OP5 share a similar region and show a resemblance to each other. However, OP2 (VP1) has a distinct clade value from the other four isolates, indicating no similarity.

The isolates were initially short-listed based on sequence similarity. The OP3, OP4, and OP5 (VP2) isolates exhibited identical sequences, whereas the OP1 (VP2) isolate showed variation. To predict the 3D structure of the protein, homology modelling, Ab-initio, and threading techniques were employed, as detailed in **Table 1**. The 3D structures of VP2 and VP1 were modelled using a structure template in the homology modelling process. The predicted structure demonstrated high accuracy, particularly at the protein's active site.[18,21]

Molecular docking was conducted using Pyrx. A comprehensive comparative docking analysis of the interactions between VP1, VP2, and selected ligands highlighted the most effective interactions with the lowest binding energy. The selected binding affinities for the ligands were 10.5 and 10.6, indicating favorable interactions between the ligands and the protein, as illustrated in **Figure 6** and **Figure 7**, **Figure 8**.[22] The interaction between the protein and ligand can pose challenges in vaccine development because the interaction between the molecules is short.

The physicochemical properties of all isolates were assessed using Expasy Prot. Parameters will be used to examine protein stability and other characteristics. VP1 demonstrated stability in terms of half-life, while OP3-VP2 exhibited more excellent stability when considering different parameters. The results indicate that VP1 is hydrophilic, whereas VP2 isolates are hydrophobic, as detailed.

The evaluation of protein allergenicity and antigenicity revealed that OP1-VP2 is classified as an allergen and an antigen, indicating its potential to elicit immune responses and allergic reactions. Conversely, OP2-VP1 is neither an antigen nor an allergen, suggesting a low likelihood of triggering an immunological response or allergic reaction. OP3-VP2 can induce an immune response without eliciting an allergic reaction as an antigen but not an allergen. These findings have significant implications for our understanding of the diverse immunological profiles of the proteins.

All three isolates' molecular dynamics simulation results demonstrate consistent protein and ligand stability throughout the 20 nanosecond simulation. The OP1-VP2 isolate exhibits sustained stability and strong interaction between the ligand and protein, characterized by abundant beta-sheets and notable hydrophobic and hydrogen interactions. Conversely, the OP2-VP1 isolate displays shorter interaction periods compared to OP1-VP2. Still, it maintains good stability, with alpha helices and beta sheets indicated by the percentage of secondary structure elements (SSE). Hydrogen and hydrophobic interactions are observed in this case as well. The OP3-VP2 isolate shows comparatively lower interaction levels than the other two isolates, with the interaction graph indicating hydrogen and hydrophobic interactions. The percentage SSE suggests a significant presence of beta sheets, with no alpha helices, which play a crucial role in maintaining overall structural stability (Liu *et al*., 2015).

10. Conclusion

This study comprehensively analyzed the interactions between three specific compounds: OP2-VP1, OP1-VP2, and OP3-VP2. Among these compounds, OP2-VP1 emerged with the most favorable half-life, indicating a longer duration of stability in the biological environment. Despite its promising interaction characteristics during simulation, OP2-VP1 was inherently unstable and lacked significant antigenic qualities, which are crucial for immune response. In contrast, OP1-VP2, although having a comparatively shorter half-life, showcased remarkable stability in its aliphatic index. This compound demonstrated superior interaction dynamics in simulations, outperforming all other studied compounds, and possessed both antigenic and allergenic properties, making it a more versatile candidate. Meanwhile, OP3-VP2 exhibited a stable interaction profile and maintained a longer half-life than OP1-VP2. However, it fell short regarding the aliphatic index stability and did not display any allergenic properties. Considering all these factors, the study concluded that OP1-VP2 stands out as the most promising option among the proteins examined due to its stability, interaction quality, and desirable biological attributes.

11. Source of Funding

None.

12. Conflict of Interest

None.

References

1. Liu M. Vakharia VP. Protein of infectious bursal disease virus modulates the virulence in vivo. *Virology*, 2004. 330(1): p. 62–73.
2. Dey S. Infectious bursal disease virus in chickens: prevalence, impact, and management strategies. *Vet Med (Auckl)*. 2019:85–97.
3. Mahgoub H.A.J. A.o.v., An overview of infectious bursal disease. 2012. *Arch Virol* 157:(11):2047–57.
4. Sharma J.M. Infectious bursal disease virus of chickens: pathogenesis and immunosuppression. *J Integrat Agricul*. 2000; 24:(2-3):223–35.
5. Aliyu H.B. Genetic diversity of recent infectious bursal disease viruses isolated from vaccinated poultry flocks in Malaysia. 2021. 8: p. 643976.
6. Wang Y.-L. An improved scheme for infectious bursal disease virus genotype classification based on both genome segments A and B. 2021; 20(5): 1372–81.
7. Yuan L. Microbiota in viral infection and disease in humans and farm animals. *Prog Mol Biol Transl Sci*. 2000;171(5):15–60.
8. Kibenge F.S., Dhillon A. R.J.J.o G.V. Russell, Biochemistry and immunology of infectious bursal disease virus. *J Gen Virol*, 1988. 69(8):1757–75.
9. Dey S. Infectious bursal disease virus in chickens: prevalence, impact, and management strategies. *Vet Med (Auckl)*:2019;10:85–97.
10. Soleymani S., Janati-Fard F, Housaindokht MR., Designing a bioadjuvant candidate vaccine targeting infectious bursal disease virus (IBDV) using viral VP2 fusion and chicken IL-2 antigenic epitope: A bioinformatics approach. *Comput Biol Med*, 2023. 163:107087.

11. Huycke M.M., Sahm DF, Gilmore MS, Multiple-drug resistant enterococci: the nature of the problem and an agenda for the future. *Emerg Infect Dis*. 1998;4(2):239–49.
12. Rasheed, M.A. Identification of lead compounds against Scm (fms10) in Enterococcus faecium using computer-aided drug designing. *Life (Basel)*. 2021;11:(2):77.
13. Ou C. Transcription profiles of the responses of chicken bursae of Fabricius to IBDV in different timing phases. *Virol J*. 2017;14(1): p. 93.
14. Xu G. Complete Genome Characterization of a Novel Infectious Bursal Disease Virus Strain Isolated from a Chicken Farm in China. *Microb Resour Announc*, 2019:(48):e00632–19
15. UniProt: a worldwide hub of protein knowledge. *Nucleic Acids Res*, 2019; 47(1):D506–15.
16. Ebrahimi M. Recombinant VP2 expressed in baculovirus and adjuvanted with TIR-]'TLR7: a vaccine candidate against infectious bursal disease virus. 2018;27(4):911–6.
17. Daina A., O. Michielin, V. Zoete, SwissADME: a free web tool to evaluate pharmacokinetics,'drug-likeness and medicinal chemistry friendliness of small molecules. *Sci Rep*. 2017;7(2):42717.
18. Bowers K. Molecular dynamics—Scalable algorithms for molecular dynamics simulations on commodity clusters. Supercomputing, 2006. SC'06. 2006. 84.
19. Shivakumar D. Prediction of Absolute Solvation Free Energies using Molecular Dynamics Free Energy Perturbation and the OPLS Force Field. *J Chem Theory Comp*. 2010;6(5):1509–19.
20. Liu D. Molecular characterisation and phylogenetic analysis of infectious bursal disease viruses isolated from chicken in South China in 2011. 2013. 45:(5):1107–12.
21. Soleymani S. Designing a bioadjuvant candidate vaccine targeting infectious bursal disease virus (IBDV) using viral VP2 fusion and chicken IL-2 antigenic epitope: A bioinformatics approach. *Comput Biol Med*. 2023;163:107087.
22. Gul I. A multiepitope vaccine candidate against infectious bursal disease virus using immunoinformatics-based reverse vaccinology approach. *Front Vet Sci*. 2023;9(6):1116400.
23. Li Z. Molecular characteristics and evolutionary analysis of a virulent infectious bursal disease virus. 2015. *Sci China Life Sci*. 58:(8):731–8.

Cite this article: Mehmood MD, Ali E, Ul-Haq HA,Habib R, Ismail M, Arshed F. Decoding the enigma of bursal disease virus: Unraveling the complex interactions of proteins and molecules for enduring stability. *Int J Clin Biochem Res*. 2025;12(1):42-50.